

## Description of chemical reactions in terms of the properties of the electron density

Elfi Kraka and Dieter Cremer

*Theoretical Chemistry, University of Göteborg, Kemigården 3, S-41296 Göteborg (Sweden)*

(Received 29 May 1991)

### Abstract

Chemical reactions can be described by utilizing the topological features of the electron density distribution  $\rho(\mathbf{r})$ . This implies defining atoms in molecules, chemical bonds, molecular graphs, molecular structure, structural stability, and changes in molecular structure from a topological point of view. Looked at in this way, chemical reactions are transitions from one structural region to another passing through one or several unstable structures, which can be associated with the transition state(s) of chemical reactions. An alternative way of describing chemical reactions is given by the analysis of the Laplace concentration  $-\nabla^2\rho(\mathbf{r})$ . This leads to a more qualitative account of changes in molecular structure owing to chemical reactions. It also has the advantage of bridging the gap between molecular-orbital-based and  $\rho(\mathbf{r})$ -based descriptions of chemical reactions and molecular activity.

### INTRODUCTION

Many heuristic models and concepts used to describe chemical reactions are based on molecular orbital (MO) theory [1]. Therefore, it is not surprising that most chemists prefer to explain bond-breaking and bond-forming processes in terms of the accompanying changes of the MOs. These descriptions are often easy to understand but mostly very difficult to verify on a quantitative basis. This is because MOs (as well as atomic orbitals (AOs)) are non-observable. Furthermore, MOs can be transformed in many ways (applying appropriate unitary transformations) without changing the energy, geometry or other observable properties of the molecule in question. It often occurs that a certain reaction of the molecule can easily be rationalized with one set of MOs (e.g. delocalized MOs), while it is difficult to understand if a transformed set of MOs (e.g. localized MOs) is used.

To describe bond-breaking and bond-forming processes in terms of MOs implies that chemical bonding can be defined or at least rationalized in terms of MOs. While this seems to be straightforward in cases such as  $\text{H}_2$  or  $\text{He}_2$  it becomes very complicated and almost impossible if chemical bonding in polyatomic molecules has to be explained [2]. A simple example may illustrate

this. Homoaromaticity is believed to arise from through-space overlap between  $p\pi$  orbitals of two carbon atoms separated by a saturated  $\text{CH}_2$  group [3]. Since the interacting centres are normally separated by 1.8–2.2 Å [4], the orbital overlap is actually very small. Therefore, the key question of homoaromaticity is whether a small orbital overlap can lead to a homoaromatic C–C bond. It is clear that such a question cannot be answered in a general way. Similarly, it is impossible to derive from MO theory whether a bond is broken at the same time before, or after the transition state of a bond-breaking reaction [5].

In view of these disadvantages of MO descriptions of chemical reactions, it seems to be better to abandon orbitals and to use other means of describing molecules and molecular reactivity. Of course, from a theoretical point of view, the universal descriptor of reacting or non-reacting molecules is the molecular wavefunction  $\Psi$ . The wavefunction  $\Psi$  embodies all the information about the structure, stability, and reactivity of a molecule. However, it contains this information in a complex form that is difficult to translate into easy to understand descriptions of molecular reactions. Therefore, it is better to use a molecular quantity that is: (a) a function of  $\Psi$ , (b) invariant under unitary transformations of the MOs, (c) an observable molecular property, (d) directly related to the molecular energy and other molecular properties, and (e) useful in describing atoms in molecules and chemical bonding. Such a quantity would definitely be more suitable for the description and rationalization of chemical reactions.

One quantity that fulfils requirements (a) to (e) is the total one-electron density distribution  $\rho(\mathbf{r})$ . It is (a) a direct function of  $\Psi$ , (b) invariant with regard to unitary transformations of the MOs, and (c) an observable molecular property. Furthermore, Hohenberg and Kohn [6] have shown that the energy of a non-degenerate electronic ground state of a molecule is a unique functional of  $\rho(\mathbf{r})$ , which implies that (d) other chemical and physical properties can also be related to  $\rho(\mathbf{r})$ .

The properties of  $\rho(\mathbf{r})$  can be used to dissect the molecular space into atomic subspaces. Bader and co-workers [7] have developed the virial partitioning method, which leads to well-defined subspaces in which the virial theorem and other quantum mechanical laws are valid in the same way as they are in the total molecular space. Experience shows that in most cases (but not all [8]) there is just one nucleus located in a virial subspace. Hence, the virial partitioning method is a unique way of dissecting  $\rho(\mathbf{r})$ , which can be used:

- (i) to develop a model description of atoms in molecules;
- (ii) to develop a  $\rho(\mathbf{r})$ -based model of chemical bonding;
- (iii) to define molecular structure in terms of the topology of  $\rho(\mathbf{r})$ ;
- (iv) to describe chemical reactions as changes in the topology of  $\rho(\mathbf{r})$ .

(For recent reviews see refs. 5 and 7.)

Following (i) to (iv) it is, in principle, possible to describe any chemical reaction. This is discussed in the following section using some examples. As

we will see, this approach has its advantages and disadvantages, the latter have to do with the fact that the association of the virial subspaces with atomic subspaces is only a model and not an exact theory.

Because of these disadvantages, it is often better to use other properties of  $\rho(\mathbf{r})$  as descriptors for the molecular changes that occur during a reaction. In this respect, the Laplacian of the electron density is very promising [9,10]. It leads to simple descriptions of and insights into chemical reactions without the need for computer-time-demanding partitioning techniques of  $\rho(\mathbf{r})$ . Therefore, we will describe the Laplacian of  $\rho(\mathbf{r})$  and demonstrate its usefulness for qualitative descriptions of chemical reactions later in this paper.

## CHEMICAL BONDING, MOLECULAR STRUCTURE, AND CHANGES IN MOLECULAR STRUCTURE

Two bonded atoms A and B are connected by a path of maximum electron density (MED) [7]. Any lateral displacement from the MED path leads to a decrease in  $\rho(\mathbf{r})$ . Coming from A,  $\rho(\mathbf{r})$  first decreases until it reaches a minimum. This minimum of  $\rho(\mathbf{r})$  along the MED path is actually a saddle point  $\mathbf{r}_b$  in three dimensions. The point  $\mathbf{r}_b$  is located in the surface (zero-flux surface [7]) which separates the virial subspace of A from that of B. When going beyond  $\mathbf{r}_b$  the density  $\rho(\mathbf{r})$  increases towards B until it reaches a maximum. This is illustrated in Fig. 1 which shows a perspective drawing of the electron-density distribution of benzene.

The MED path can be considered to be an image of the chemical bond. However, there are also MED paths in the case of weak molecular interactions typical of van der Waals complexes [11]. In order to distinguish between covalent bonding and closed-shell interactions typical of electrostatic or ionic bonding, dispersion interactions and other non-covalent interactions, Cremer and Kraka [11,12] have suggested a necessary and a sufficient condition for covalent bonding, both conditions being based on the properties of  $\rho(\mathbf{r})$ :

(i) Covalent bonding requires an MED path between the atoms in question (necessary condition);

(ii) Covalent bonding requires that the local energy density  $H(\mathbf{r})$  at the saddle point  $\mathbf{r}_b$  (bond critical point) of the MED path becomes stabilizing ( $H(\mathbf{r}_b) < 0$ ) (sufficient condition).

This definition has proven to be useful in many descriptions of covalent bonding [13]. It can be used to derive a definition of molecular structure along the lines first suggested by Bader et al. [14]. For a given nuclear configuration, a molecule can be characterized by the topology of its MED (bond) paths and the associated saddle points  $\mathbf{r}_b$ . The network of MED (bond) paths defines a molecular graph. There exists a manifold of (topologically) equivalent molecular graphs that possess the same connectivity pattern of bond paths, but correspond to different geometries. Each class of equivalent molecular graphs rep-

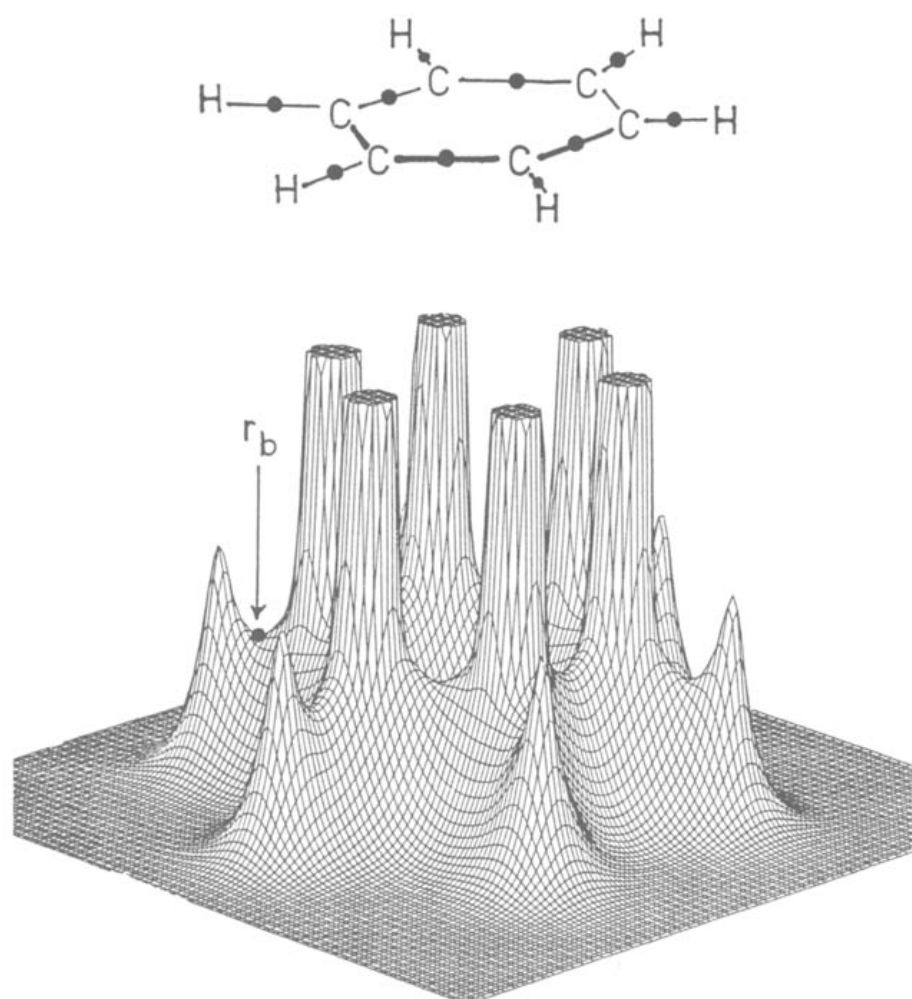


Fig. 1. Perspective drawing of the calculated electron-density distribution  $\rho(\mathbf{r})$  of benzene shown with regard to the plane containing the 12 nuclei. The position of one of the saddle points between a carbon and a hydrogen atom is marked by an arrow. The molecular graph with bond paths and bond critical points  $\mathbf{r}_b$  is shown in the upper half of the figure. For a better representation  $\rho(\mathbf{r})$  values above a threshold are cut off. (HF/6-31G(d,p) calculations.)

resents a unique molecular structure which, in turn, is associated with a structural region of the configuration space. For a molecular state, there exists a finite number of classes of equivalent graphs (molecular structures) and associated structural regions [14].

For a given system made up of a finite number of atoms, the collection of all structural regions together with their boundaries is called a structure diagram. Any process that leads the system from one structural region to another is a chemical reaction. Any process that leads the system outside its structural diagram into another diagram implies a change in the number of atoms and, therefore, is no longer a chemical reaction but an atom (nucleus) destroying or forming process. In view of this, the structure diagram of a given system should embody all the information concerning the chemical reactions of the system in question. Accordingly, the description of chemical reactions and the elucidation of reaction mechanisms should be based on changes in the topology of the bond critical points of  $\rho(\mathbf{r})$  (changes in the molecular graph) and on the corresponding transitions from one region of the structure diagram to another.

The usefulness of these definitions may be explained with the help of an

example. For this purpose we consider the three-atom system ABC. A priori, one would predict that this system possesses four structural regions corresponding to the molecular structures I-IV.



There are two bond paths for I, II, and III, but three for IV, which represents a three-membered ring. The first three structures comprise linear as well as bent molecular graphs (geometries), but for reasons of simplicity we consider here only the linear molecular graphs.

The actual structure diagram (Fig. 2) shows 10 structural regions, but only four of them (I-IV) are regions of (topologically) stable structures. The other regions (V-X) contain (topologically) unstable structures. (In a topological sense, a molecular structure is stable (unstable) if a differential change in geometry does not lead (leads) to a discontinuous change in the molecular graph. See ref. 15.) For example, structure V (see Fig. 2) is unusual due to the fact that A is no longer bonded to either B or C, but to the bond critical point of the bond B-C. This is the structure of a  $\pi$  complex and, therefore, structures V, VI and VII correspond to three different  $\pi$  complexes of the atom ensemble ABC.

In structure V, an extremely small movement of A in the direction of C (B) leads to a sudden switch of the A, (BC) path to nucleus C (B) and the formation of the stable structure BCA (ABC). Since extremely small movements of the apex atom can lead to immediate formation of a new stable structure,

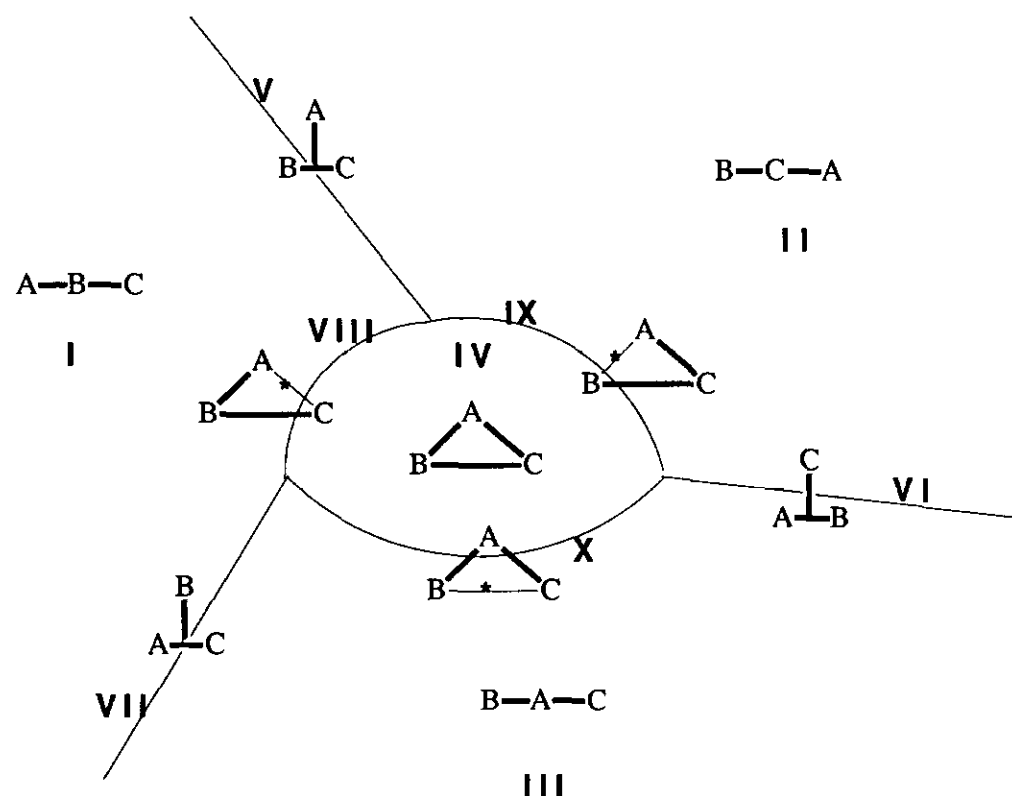
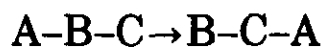


Fig. 2. Schematic representation of the structure diagram of the molecular system ABC. For each of the structural regions I-X a molecular graph is given. Asterisks denote catastrophe points.

structures such as V, VI or VII are called unstable structures. Catastrophe theory describes these structures as catastrophes of the conflict type [15].

Structures VIII, IX and X are unstable structures for the same reason, but they are characterized by the formation (or loss) of a new bond path. This is indicated by the singularity of  $\rho(\mathbf{r})$  at the position indicated by an asterisk in Fig. 2. In catastrophe theory, the points labeled by an asterisk are called bifurcation points [15]. In the structure diagram of ABC, the bifurcation point indicates the transition from an open structure to a ring structure (Fig. 2).

A chemical reaction such as the isomerization reaction



can be described in terms of structural changes as shown in Fig. 3(a). Inspection of the structure diagram reveals that there are two possible reaction paths

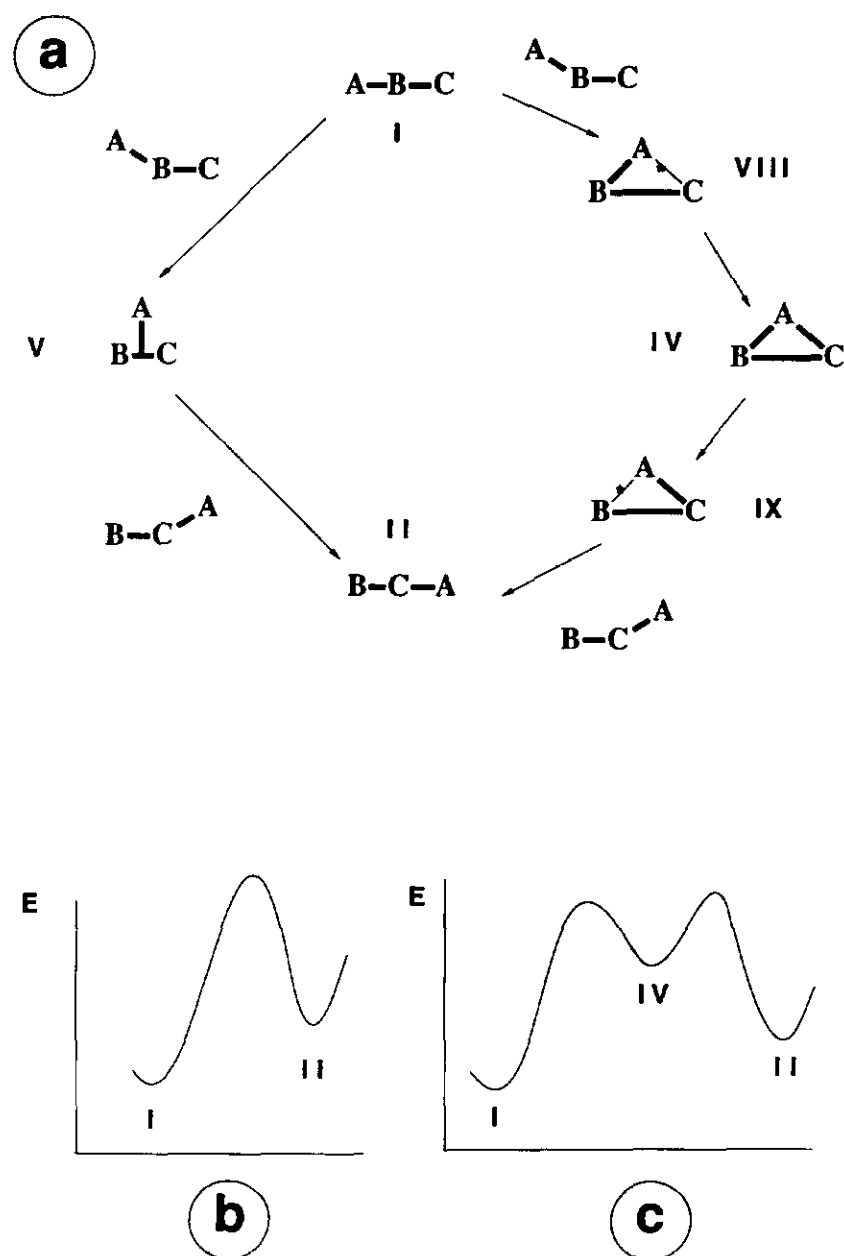


Fig. 3. Isomerization of ABC. (a) Description of possible reaction paths in terms of the molecular structures encountered along the path (compare with Fig. 2). (b,c) Possible energy profiles corresponding to the two reactions shown in (a).

for the isomerization. The first starts with a bending of the linear geometry (graph) within the structural region I. It then proceeds via the  $\pi$  complex V and enters the structural region II.

The second reaction path leads through the structural region IV, which means there are now two structural changes, one when crossing VIII and the other when crossing IX. As the ring structure IV is a stable structure (with regard to  $\rho(\mathbf{r})$ ) it is tempting to consider IV as an intermediate (with regard to the energy  $E$ ) of the isomerization reaction. Accordingly, the energetics of the two reaction paths of the isomerization can be qualitatively described by energy profiles such as those shown Figs. 3(b) and 3(c).

It is appealing to associate the unstable structures V, VIII and IX with the transition states of the two reaction paths depicted in Fig. 3(a). So far, we have investigated only a limited number of reactions (E. Kraka and D. Cremer, unpublished results). Results show that there may indeed be a one-to-one relationship between catastrophe points (unstable structures) and transition states crossed in a reaction. However, in no case investigated are the coordinates of the transition state identical with those of the corresponding catastrophe point.

An association of unstable structures and transition stages is not meaningful in those cases where the definition of atoms in molecules no longer applies, because there are more (or less) subspaces than atoms in a molecular system. For example, for  $\text{Li}_2$  three subspaces have been found as well as a relatively complicated structure diagram (with various catastrophe points) [8d] that has no bearing on the chemistry of the molecule. In these cases, one should remember the model character of the approach and refrain from speculation about unusual bonding mechanism or unusual chemical reactivity.

Apart from this, a caveat is necessary to avoid confusion about the use of the terms "structure" and "stability" within the context of a  $\rho(\mathbf{r})$ -based description of chemical reactions. These terms are normally used with regard to the properties of the molecular energy and, then, they have a completely different meaning. Stability, in a topological sense, does not necessarily imply thermodynamic (or kinetic) stability. Also, reaction intermediates may possess different topological structures but, as their energies (stabilities) or other molecular properties are the same, a chemical differentiation (within experimental accuracy) may not be possible. As long as the energetics of a given system are not determined, it does not help an experimentalist very much if he knows that a particular molecular structure is topologically stable. Predictions can be made on the basis of structure diagrams, but research is a long way off understanding the relationship between  $\rho(\mathbf{r})$ -based and  $E$ -based descriptions of structure, stability, and reactivity.

In view of the different meanings of the terms structure and stability, the use of the term " $\pi$  complex" in connection with the structure diagram in Fig. 2 is much more limited than its normal chemical use. Here, it denotes a T-

shaped molecular graph with just two bond paths. General use of the term  $\pi$  complex, however, can cover topological  $\pi$  complexes as well as three-membered rings with large  $\pi$ -complex character owing to inwardly curved bond paths [16]. In this way, a  $\pi$ -complex could also turn out to be an intermediate rather than a conflict structure (transition state).

In general, calculation of a structure diagram is costly and requires a number of steps. First, the electron density distribution  $\rho(\mathbf{r})$  has to be computed for a large number of nuclear configurations. There is no algorithm that leads to a direct location of the regions of unstable structures that separate the regions of stable structures. Accordingly, the search for the unstable structures in the configuration space has to be done by trial and error. This is much more costly than a direct transition-state search with analytical energy gradient techniques.

Furthermore, there are no time savings when focusing calculations on  $\rho(\mathbf{r})$  rather than the molecular energy  $E$ . The bond paths and molecular graphs of the unstable structures are sensitive to correlation and basis-sets effects. Therefore, correlation-corrected ab initio methods and large basis sets have to be used to make sure that all unstable structures are correctly described. This implies the calculation of response densities [17], which is best done by utilizing analytical energy gradient techniques [18]. In general, the calculation of response densities with these techniques is two to three times as costly as an energy calculation [18]. Once the response density distribution  $\rho(\mathbf{r})$  has been determined with the correlation-corrected method for a given geometry, the location of the bond paths and the molecular graph takes a matter of seconds compared to a Mulliken population analysis [5]. Hence, the real cost factor is the trial-and-error search for the unstable structures. Research is needed to develop new searching algorithms that cut down costs.

Of course there are cases where the determination of the structure diagram can be achieved because of symmetry. For example, Bader et al. [19] have calculated the structure diagram for the system O-H<sub>2</sub> (imposing  $C_{2v}$  symmetry). In a similar way Cremer and Kraka [16] have investigated the ring formation of several ABA systems. However, in general, the determination of a structure diagram with all its possible unstable structures is much more costly than direct calculation of the corresponding transition states.

#### DESCRIPTION OF CHEMICAL REACTIONS BY MEANS OF THE LAPLACIAN OF $\rho(\mathbf{r})$

One of the goals of theoretical chemistry is to predict the reactive behavior of molecules from the properties of the potential reactants. This approach is very economic and has been successfully applied on the basis of MO theory [1] (see for example the results of Hückel MO, frontier orbital, PMO, or orbital symmetry conversation theory). In the following we describe a similar approach using the Laplacian of the electron density distribution  $\rho(\mathbf{r})$ . The



Laplacian can be used to determine the electronic structure of molecules and to identify the reactive sites in a molecule [5,9].

It has been shown that the Laplacian of  $\rho(\mathbf{r})$ ,  $\nabla^2\rho(\mathbf{r})$ , reveals where electrons are concentrated ( $\nabla^2\rho(\mathbf{r}) < 0$ ) or depleted ( $\nabla^2\rho(\mathbf{r}) > 0$ ) in the molecule [9,20]. Therefore, the function  $-\nabla^2\rho(\mathbf{r})$  has been called the Laplace concentration of the electrons. The Laplace concentration possesses the important property to give zero when integrated over the molecular space or an (atomic) subspace. All fluctuations in  $-\nabla^2\rho(\mathbf{r})$  are such that local depletion or concentration of electronic charge cancel each other out for an individual atom in the molecule (defined by its virial subspace) as well as for the total molecule. If electrons concentrate at, for example, the position of a lone pair, negative charge will be depleted at another site of the molecule. In this way the Laplace concentration reveals positions of preferential electrophilic or nucleophilic attack in the molecule.

In Figs. 4 and 5, perspective drawings of both  $\rho(\mathbf{r})$  and  $-\nabla^2\rho(\mathbf{r})$  are shown for the protonation of  $\text{CN}^-$  to give HCN or HNC.



Simple Lewis structures suggest that the formation of HNC requires a considerable change in the electronic structure of the  $\text{CN}^-$  anion while the formation of HCN does not. Also, it is well known that HCN is thermodynamically more stable than HNC [21]. However, inspection of  $\rho(\mathbf{r})$  does not reveal any differences in the CN part for  $\text{H}^+$  approaching either the carbon or the nitrogen side. The electron distribution of CN seems to be (qualitatively) unchanged when going from  $\text{CN}^-$  to HCN or HNC. Not much can be said about the two reactions if the description is based on the qualitative features of  $\rho(\mathbf{r})$  alone. A quantitative analysis of  $\rho(\mathbf{r})$  is needed to describe the protonation reactions.

The case is different for  $-\nabla^2\rho(\mathbf{r})$ , which possesses a more complex structure than  $\rho(\mathbf{r})$ . Perspective drawings as well as contour-line diagrams of calculated Laplace concentrations (see Fig. 5) show that there are spheres of charge concentration and charge depletion surrounding each atom in a molecule. These spheres have been associated with the inner core and the valence shell of the atoms [9]. In a molecule the spheres are distorted in typical ways which provide insight into its electronic structure and bonding pattern [5]. For example, in the case of the cyanide anion (Figs. 5(a) and 5(b)), the concentration lumps of  $-\nabla^2\rho(\mathbf{r})$  can be associated with the inner shell electron pairs (1s), bond electron pairs (bp), and the electron lone pairs (lp) at the nitrogen and the carbon atom.

An electrophilic attack by a proton will occur at a position that offers a maximum concentration of electrons such as the site of the nitrogen or carbon lone pair. Concentration of negative charge due to the nitrogen lone pair is

almost three times as large as that due to the carbon lone pair and, therefore, one should expect an electrophile to prefer the nitrogen side and to form isocyanides. However, Fig. 5(b), which gives the contour-line diagram of the Laplace concentration of the cyanide anion (concentration is indicated by dashed contour lines), reveals another important property of the two lone-pair con-

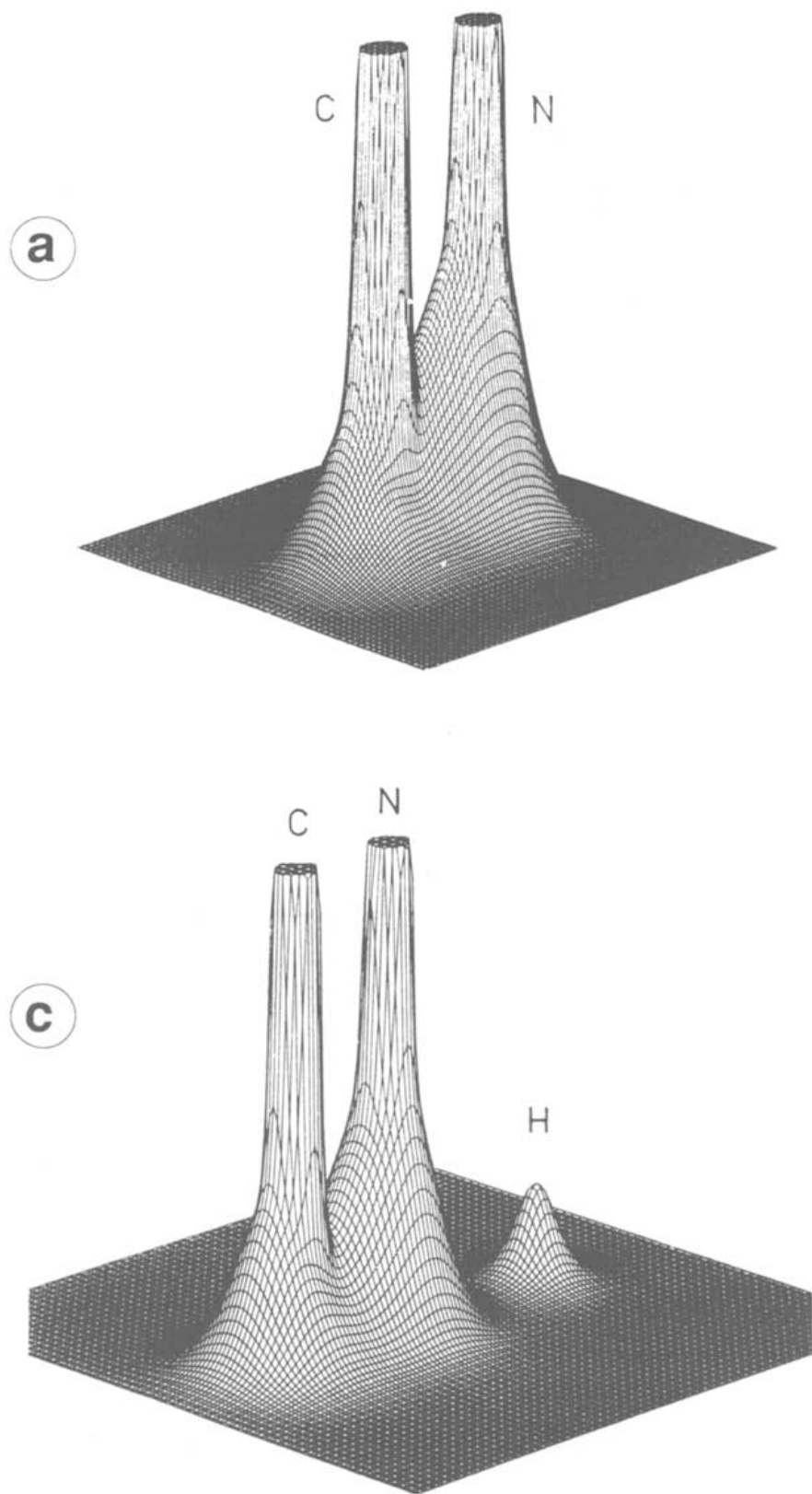


Fig. 4 (opposite and above). Perspective drawing of the calculated electron density distribution  $\rho(\mathbf{r})$  of (a)  $\text{CN}^-$ , (b)  $\text{H}^+$  approaching  $\text{CN}^-$  at the carbon side at a distance of 2 Å, (c)  $\text{H}^+$  approaching  $\text{CN}^-$  at the nitrogen side at a distance of 2 Å, and (d) HCN. For a better representation the  $\rho(\mathbf{r})$  values above a threshold have been cut off. (HF/6-31G(d,p) calculations.)

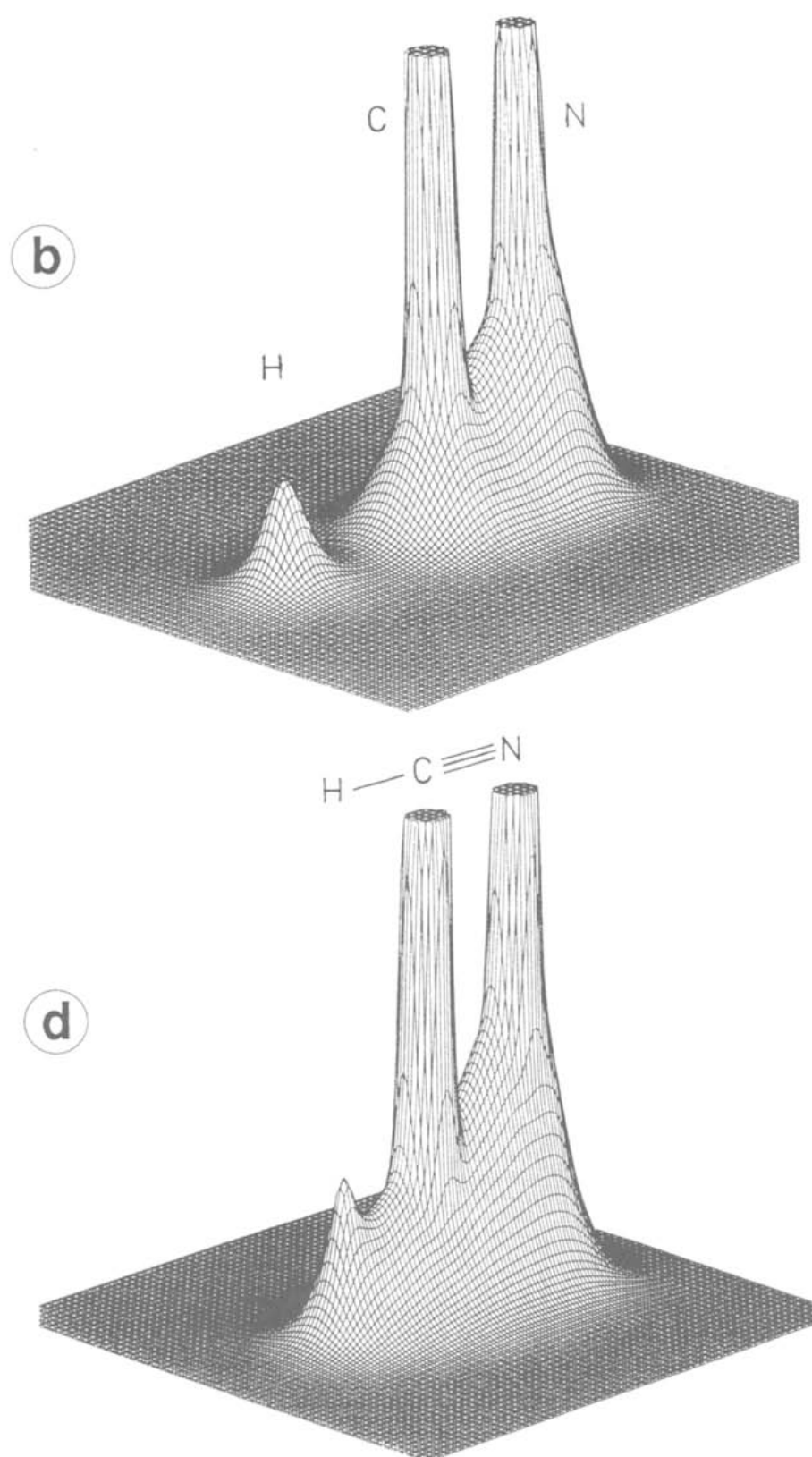


Fig. 4.

centrations. The electron lone pair at carbon is much more diffuse and extends more into space than the electron lone pair at nitrogen, which is not surprising in view of the difference in electronegativities between the two atoms.

Hence the Laplace concentration describes the cyanide anion as an ambident nucleophile with a hard end (nitrogen) and a soft end (carbon). A hard electrophile such as the proton will prefer the nitrogen lone pair while a soft electrophile will prefer the carbon lone pair according to the hard-soft acid-base concept [22]. In the first case, electrostatic interactions between the large

concentration of negative charge at nitrogen and the positive proton will dominate the reaction mechanism, while in the latter case orbital overlap will be important. It is clear that the more extended the lone pair is the more easily a reaction with a soft electrophile can take place.

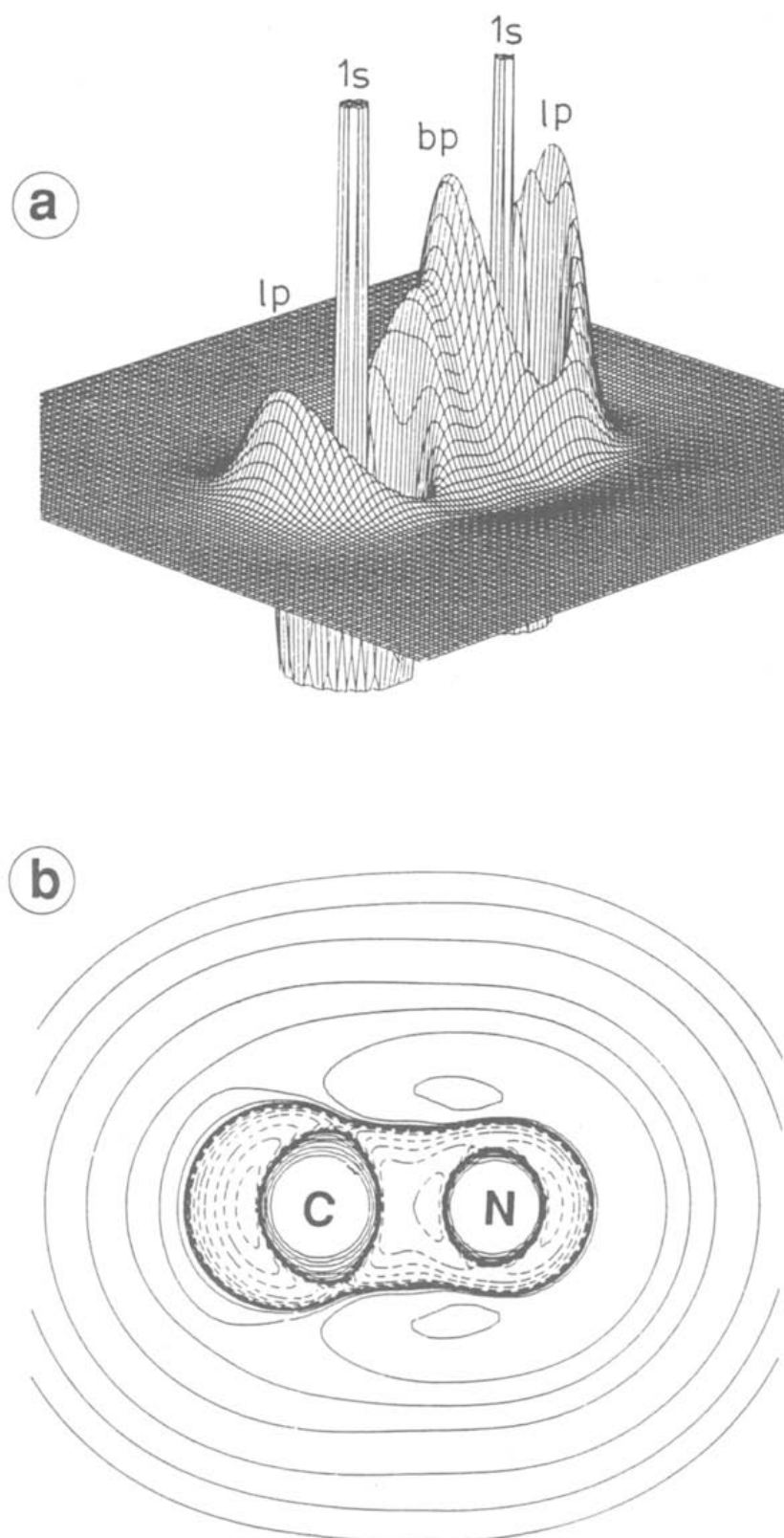
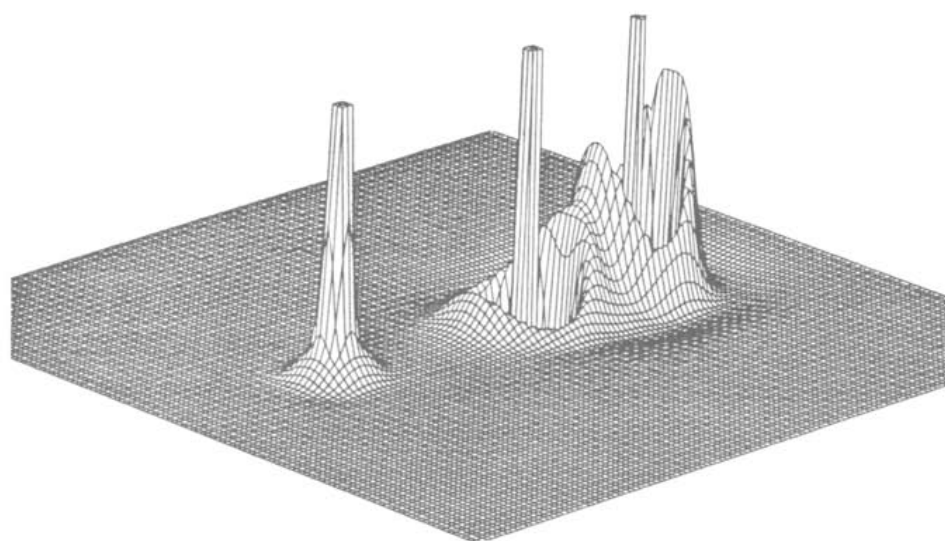


Fig. 5 (overleaf, opposite and above). Perspective drawings and contour-line diagrams of the Laplace concentration  $-\nabla^2\rho(\mathbf{r})$  of (a, b)  $\text{CN}^-$ , (c, d)  $\text{H}^+$  approaching  $\text{CN}^-$  at the carbon side at a distance of  $2 \text{ \AA}$ , (e, f)  $\text{H}^+$  approaching  $\text{CN}^-$  at the nitrogen side at a distance of  $2 \text{ \AA}$ , and (g, h)  $\text{HCN}$ . Inner shell (1s), bond (bp), and lone pair (lp) concentrations are indicated in the perspective drawings of  $-\nabla^2\rho(\mathbf{r})$  of  $\text{CN}^-$  and  $\text{HCN}$ . Laplace values above and below a threshold value have been cut off. In the contour-line diagrams, inner-shell concentrations are not shown (HF/6-31G(d,p) calculations.)

According to this description one would expect that protonation (e.g. by HCl or HBr) exclusively leads to HNC, while in reality the opposite is true [23]. This, of course, has to do with the larger thermodynamic stability of HCN, which in the gas phase is about 10–15 kcal mol<sup>-1</sup> more stable than HNC [21]. This difference in stability is reflected by perspective drawings of the Laplace concentrations of a proton approaching CN<sup>-</sup> at either the carbon (Fig. 5(c)) or the nitrogen side (Fig. 5(e)) at a distance of 2 Å. In Figs. 5(d) and 5(f) the corresponding contour-line diagrams of  $-\nabla^2\rho(\mathbf{r})$  are shown. In the first case, the lone pair concentration is pulled out in the direction of the proton, thus lowering its maximum value. Figure 5(d) shows that electronic charge starts

(c)



(d)

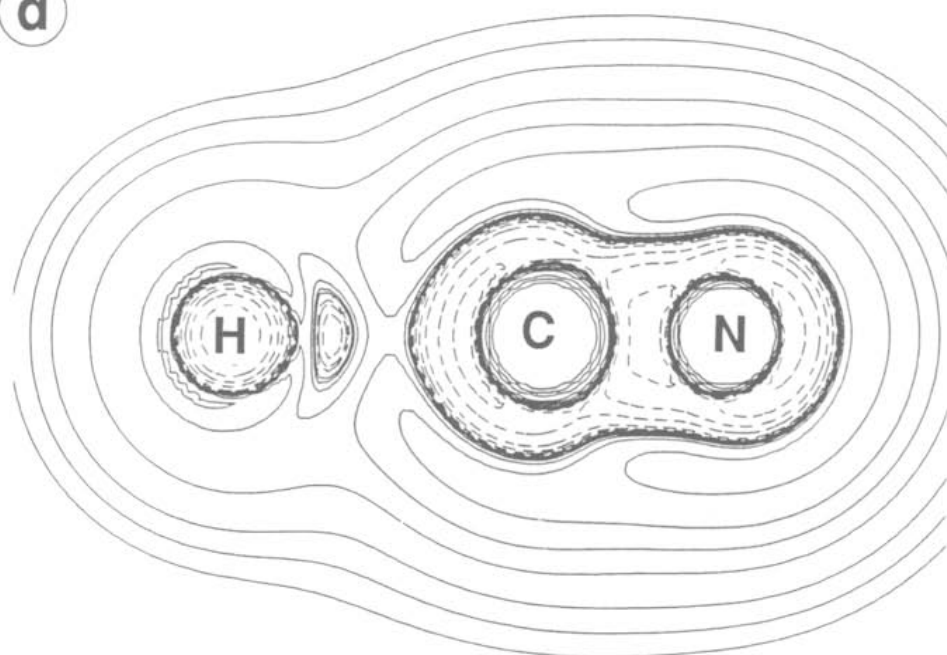
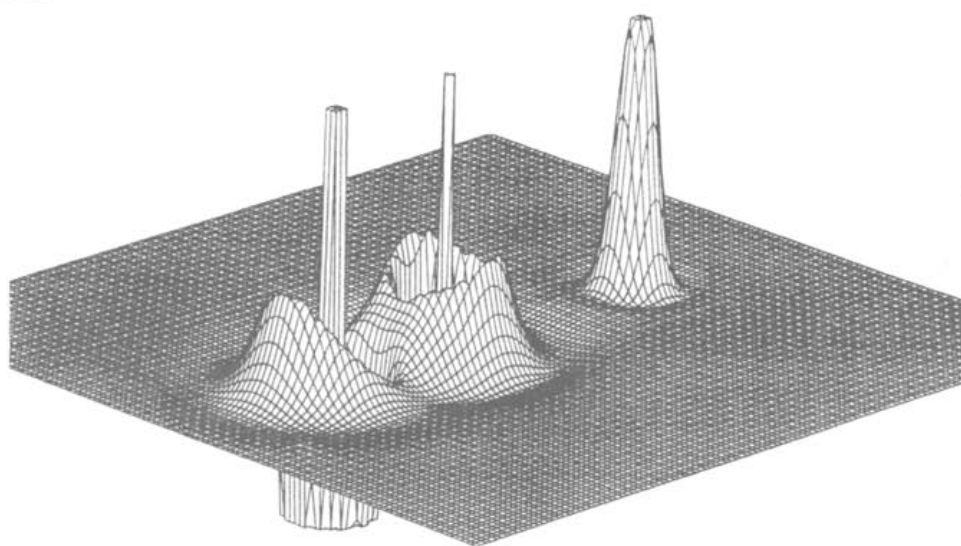


Fig. 5 (continued).

to concentrate between the hydrogen and carbon atoms to form a C–H bond. At the same time the charge concentration at the nitrogen atom is pulled in the direction of the carbon atom, which means that the lone pair concentration at nitrogen is contracted, thus increasing its maximum value. There are, however, no significant changes in the C–N bond region.

Attack of the proton at the nitrogen side of  $\text{CN}^-$  does not lead to a distortion of lone pair concentration toward  $\text{H}^+$  (Figs. 5(e) and 5(f)). It seems that the nitrogen lone pair is too “hard” to be easily distorted to an N–H bond concentration and, therefore, the N–H bond concentration seems to be formed at a later stage than the C–H bond concentration. Instead, the Laplace concentration in the valence sphere of nitrogen rearranges (Fig. 5(e)). The concentra-

e



f

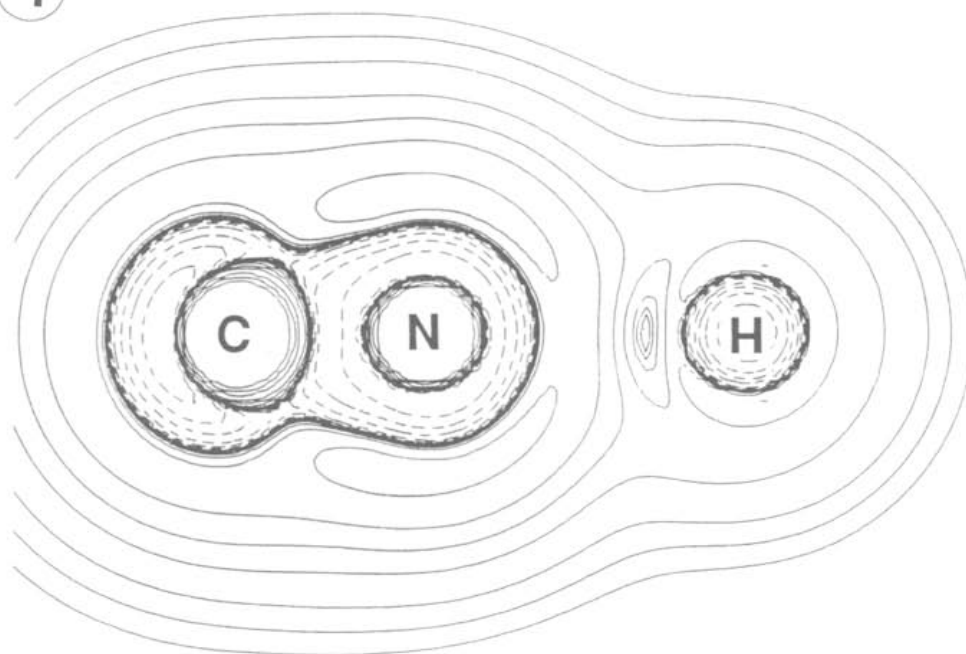
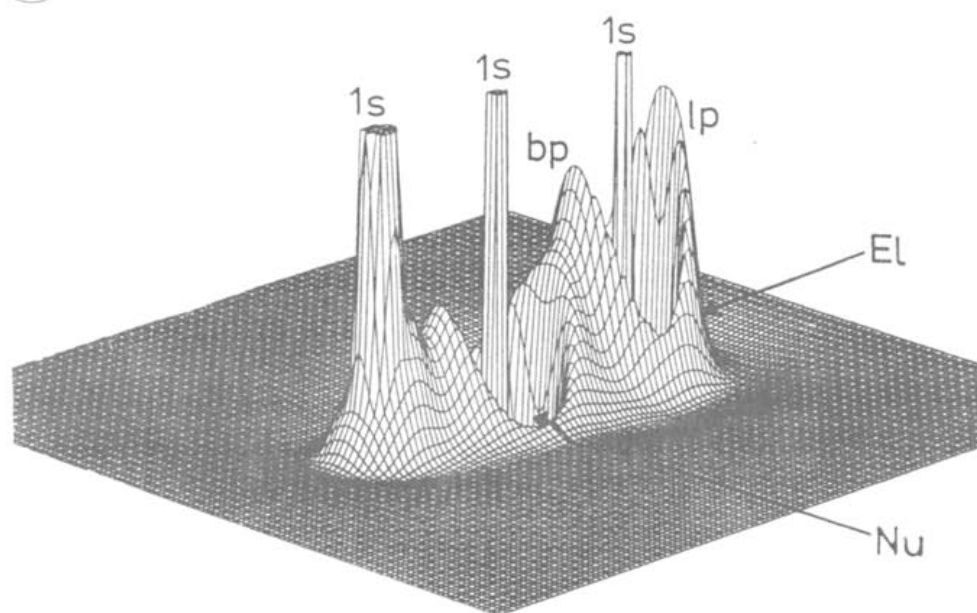


Fig. 5 (continued).

tion lumps before and behind the nitrogen atom in the direction of the C–N axis are reduced, while new concentration lumps emerge in the direction perpendicular to the C–N axis, i.e. in the  $\pi$  region. This is exactly that what one would expect in view of the Lewis structure of HNC (see above). As a consequence of the reorganization of the Laplace concentration of CN, the nitrogen nucleus is deshielded in the direction of the carbon nucleus and the C–N nuclear repulsion is increased (the N–C bond length in HNC is 1.15 Å as compared to 1.13 Å in HCN). Although protonation at the nitrogen side should proceed without any barrier (both in the gas and the solution phase), the features of  $-\rho(\mathbf{r})$  suggest that the resulting product (HNC) should be less stable than HCN.

g



h

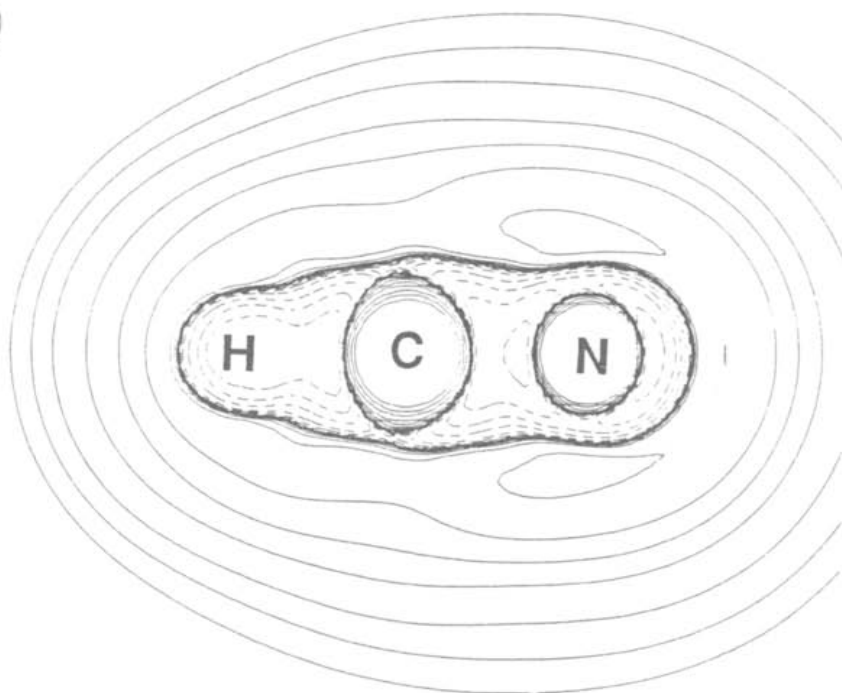
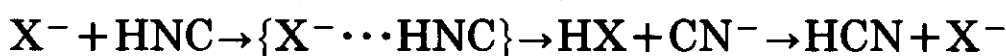


Fig. 5 (continued).

In summary, inspection of the Laplace concentration reveals that protonation should take place at the nitrogen atom, but that HCN should be the thermodynamically more stable product. Similar answers can be derived from a quantitative analysis of  $\rho(\mathbf{r})$ , but not just by inspecting graphical representations of  $\rho(\mathbf{r})$  such as those shown in Fig. 4. Of course, neither  $\rho(\mathbf{r})$  nor  $-\nabla^2\rho(\mathbf{r})$  can provide a direct answer to the question of why HCN is formed exclusively. This could be due to proton exchange reaction with either  $\text{CN}^-$  or  $\text{X}^- = \text{Cl}^-$  or  $\text{Br}^-$  acting as a catalyst.



Inspection of the perspective drawings of  $-\nabla^2\rho(\mathbf{r})$  in Fig. 5 also reveals where possible nucleophilic attacks may take place. There are distinct holes in the valence shell of HCN (Fig. 5(g)) at both carbon and nitrogen. However, the hole at the carbon atom is deeper than that at the nitrogen atom, which means that the carbon nucleus is less shielded than the nitrogen nucleus. Therefore, a nucleophile will preferentially attack at the carbon atom, in line with experimental observations.

Analysis of the Laplace concentration has helped to predict  $\text{p}K_a$  values of azaannulenes [24], to elucidate the mechanism of  $\text{S}_{\text{N}}2$  and  $\text{S}_{\text{E}}2$  reactions [5], to predict product ratios for nucleophilic and electrophilic substitution reactions of benzene [5], and to explore possible reactions of noble gas elements He, Ne, and Ar [25]. It has been stressed [5,9] that (at least for simple molecules) regions with concentration and depletion of negative charge coincide with the regions in which the highest-occupied MO (HOMO) and lowest-unoccupied MO (LUMO) possess their largest amplitude. Thus, in the same way as one predicts reactive behavior utilizing frontier orbitals, an investigation of the Laplace concentration  $-\rho(\mathbf{r})$  of a reactive molecule can be used. The analysis of the Laplace concentration provides a link between the MO approach and the electron density approach to the description of molecules and their chemical reactions. As  $\nabla^2\rho(\mathbf{r})$  covers the effects of all occupied MOs, it does not suffer from the ambiguities of frontier orbital theory with regard to the choice of the MOs to be analysed (HOMO, second HOMO, third HOMO, etc.).

#### ACKNOWLEDGEMENTS

This work was supported by the Swedish Naturvetenskapliga Forskningsrådet (NFR). All calculations were done on the CRAY XMP/48 computer of the NSC, Linköping, Sweden. The authors thank the NSC for a generous allotment of computer time.



## REFERENCES

- 1 See, for example, (a) L. Salem, *The Molecular Orbital Theory of Conjugated Systems*, Benjamin, W.A. Inc., New York, 1966.  
 (b) E. Heilbronner and H. Bock, *Das HMO-Modell und seine Anwendung—Grundlagen und Handhabung*, Verlag Chemie, Weinheim/Bergstrasse, 1968.  
 (c) M.J.S. Dewar, *The Molecular Orbital Theory of Organic Chemistry*, McGraw-Hill, New York, 1969.  
 (d) R.B. Woodward and R. Hoffmann, *Die Erhaltung der Orbitalsymmetrie*, Verlag Chemie, Weinheim, 1970.  
 (e) N.T. Anh, *Die Woodward-Hoffmann-Regeln und ihre Anwendungen*, Verlag Chemie, Weinheim, 1972.  
 (f) M.J.S. Dewar and R. Dougherty, *The PMO Theory of Organic Chemistry*, Plenum, New York, 1975.  
 (g) B.M. Gimarc, *Molecular Structure and Bonding—The Qualitative Molecular Orbital Approach*, Academic Press, New York, 1979.  
 (h) I. Fleming, *Grenzorbitale und Reaktionen Organischer Verbindungen*, Verlag Chemie, Weinheim, 1979.
- 2 (a) K. Ruedenberg, in O. Chelvet, R. Daudel, S. Diner and J.P. Malrien (Eds), *Localization and Delocalization in Quantum Chemistry*, Vol. 1, D. Reidel, Dordrecht, 1975, p. 223.  
 (b) K. Ruedenberg, *Rev. Mod. Phys.*, 34 (1962) 326.  
 (c) C. Edmiston and K. Ruedenberg, *J. Phys. Chem.*, 68 (1963) 1628.  
 (d) E.M. Layton, Jr. and K. Ruedenberg, *J. Phys. Chem.*, 68 (1963) 1654.  
 (e) R.R. Rue and K. Ruedenberg, *J. Phys. Chem.*, 68 (1963) 676.
- 3 For reviews on homoaromaticity see (a) S. Winstein, *Q. Rev. Chem. Soc.*, 23 (1969) 141.  
 (b) P.M. Warner, in T. Nozoe, R. Breslow, K. Hafner, S. Ito and I. Murata (Eds), *Topics in Nonbenzenoid Aromatic Character*, Vol. 2, Hirokawa, Tokyo, 1979.  
 (c) L.A. Paquette, *Angew. Chem., Int. Ed. Engl.*, 17 (1978) 106.  
 (d) R.F. Childs, *Acc. Chem. Res.*, 17 (1984) 347.
- 4 F. Reichel, E. Kraka and D. Cremer, *J. Am. Chem. Soc.*, in press.
- 5 E. Kraka and D. Cremer, in Z.B. Maksic (Ed.), *Theoretical Models of the Chemical Bond, Part 2: The Concept of the Chemical Bond*, Springer-Verlag, Berlin, 1990, p. 453.  
 (b) D. Cremer, in Z.B. Maksic (Ed.), *Modelling of Structure and Properties of Molecules*, Ellis Horwood, Chichester, 1988, p. 125.
- 6 P. Hohenberg and W. Kohn, *Phys. Rev. B*, 136 (1964) 864.
- 7 (a) R.F.W. Bader, T.T. Nguyen-Dang and Y. Tal, *Rep. Prog. Phys.*, 44 (1981) 893.  
 (b) R.F.W. Bader and Nguyen-Dang, T.T., *Adv. Quantum Chem.*, 14 (1981) 63.  
 (c) R.F.W. Bader in B.M. Deb (Ed.), *The Force Concept in Chemistry*, Van Nostrand Reinhold, New York, 1981, p. 39.
- 8 See, for example, (a) C. Gatti, P. Fantucci and G. Pacchioni, *Theor. Chim. Acta*, 72 (1987) 433.  
 (b) W.L. Cao, C. Gatti, P.J. MacDougall and R.F.W. Bader, *Chem. Phys. Lett.*, 141 (1987) 380.  
 (c) C. Gatti and R.F.W. Bader, *J. Chem. Phys.*, 88 (1988) 3792.  
 (d) J. Cioslowski, *J. Phys. Chem.*, 94 (1990) 5496.
- 9 (a) R.F.W. Bader and H. Essén, *J. Chem. Phys.*, 80 (1987) 1943.  
 (b) R.F.W. Bader, P.J. MacDougall and C.D.H. Lau, *J. Am. Chem. Soc.*, 106 (1984) 1594.  
 (c) R.F.W. Bader and P.J. MacDougall, *J. Am. Chem. Soc.*, 107 (1985) 6788.
- 10 E. Kraka and D. Cremer, *Z. Kristallogr.*, 170 (1985) 106.
- 11 D. Cremer and E. Kraka, *Croat. Chim. Acta*, 57 (1984) 1259.
- 12 D. Cremer and E. Kraka, *Angew. Chem. Int. Ed. Engl.*, 23 (1984) 67.

- 13 (a) D. Cremer, J. Gauss, P.v.R. Schleyer and P.H.M. Budzelaar, *Angew. Chem. Int. Ed. Engl.*, 23 (1984) 370.  
(b) D. Cremer and J. Gauss, *J. Am. Chem. Soc.*, 108 (1986) 7467.  
(c) D. Cremer and C.W. Bock, *J. Am. Chem. Soc.*, 108 (1986) 3375.  
(d) W. Koch, G. Frenking, J. Gauss, D. Cremer, A. Sawaryn and P.v.R. Schleyer, *J. Am. Chem. Soc.*, 108 (1986) 5732.  
(e) W. Koch, G. Frenking, J. Gauss and D. Cremer, *J. Am. Chem. Soc.*, 108 (1986) 5808.  
(f) P.H.M. Budzelaar, D. Cremer, M. Wallasch, E.-U. Würthwein, P.v.R. Schleyer, *J. Am. Chem. Soc.*, 109 (1987) 6290.  
(g) D. Cremer and E. Kraka, in J.F. Liebman and A. Greenberg (Eds), *Molecular Structure and Energetics, Structure and Reactivity*, Vol. 7, VCH Publishers, Deerfield Beach, FL, 1988, p. 65.  
(h) D. Cremer, *Tetrahedron*, 44 (1988) 7427.  
(i) D. Cremer, J. Gauss and E. Kraka, *J. Mol. Struct. (Theochem)*, 169 (1988) 531.
- 14 R.F.W. Bader, Y. Tal, S.G. Anderson and T.T. Nguyen-Dang, *Isr. J. Chem.*, 19 (1980) 8.
- 15 (a) R. Thom, *Structural Stability and Morphogenesis*, Benjamin-Cummings Publishing Co., Reading, MA, 1975.  
(b) T. Poston and I. Stewart, *Catastrophe Theory and its Applications*, Pitman, Boston, MA, 1981.
- 16 D. Cremer and E. Kraka, *J. Am. Chem. Soc.*, 107 (1985) 3800, 3811.
- 17 E. Kraka, J. Gauss and D. Cremer, *J. Mol. Struct. (Theochem)*, 234 (1991) 95.
- 18 See, for example, J. Gauss and D. Cremer, *Adv. Quantum Chem.*, in press.
- 19 R.F.W. Bader, T.T. Nguyen-Dang and Y. Tal, *J. Chem. Phys.*, 70 (1979) 4316.
- 20 P.M. Morse and H. Feshbach, *Methods in Theoretical Physics*, McGraw-Hill, New York, 1953, Vol. 1, p. 6.
- 21 (a) A. Maki and R. Sams, *J. Chem. Phys.*, 75 (1981) 4178.  
(b) G.L. Blackman, R.D. Brown, P.D. Godfrey and H.I. Gunn, *Chem. Phys. Lett.*, 34 (1975) 241.  
(c) C.F. Pau and W.J. Hehre, *J. Phys. Chem.*, 86 (1982) 321.
- 22 (a) R.G. Pearson, *J. Am. Chem. Soc.*, 85 (1963) 3533.  
(b) R.G. Pearson and J. Songstad, *J. Am. Chem. Soc.*, 89 (1967) 1827.
- 23 M.M. Maricq, M.A. Smith, C.J.S.M. Simpson and G.B. Ellison, *J. Chem. Phys.*, 74 (1981) 6154.
- 24 W. Tückmantel, G. Andree, A. Seidel, H. Schmickler, J. Lex, E. Kraka, M. Haug, D. Cremer and E. Vogel, *Angew. Chem.*, 97 (1985) 592; *Angew. Chem. Int. Ed. Engl.*, 24 (1985) 592.
- 25 (a) W. Koch, G. Frenking, J. Gauss, D. Cremer and J.R. Collins, *J. Am. Chem. Soc.*, 109 (1987) 5917.  
(b) G. Frenking, W. Koch, F. Reichel and D. Cremer, *J. Am. Chem. Soc.*, 112 (1990) 4240.  
(c) G. Frenking and D. Cremer, *Struct. Bonding*, 73 (1990) 17.